10-1-2008

Microstructure Analysis of Aluminum Alloy and Copper Alloy Circular Shells After Multiaxial Plastic Buckling

N. Drusina

R. Mahapatra

A. Abdul-Latif

R. Baleh

C. Wilhelm

See next page for additional authors

JMEPEG (2008) 17:755–766
DOI: 10.1007/s11665-008-9216-6

1059-9495/$19.00

Microstructure Analysis of Aluminum Alloy and Copper Alloy Circular Shells After Multiaxial Plastic Buckling

N. Drusina, R. Mahapatra, A. Abdul-Latif, R. Baleh, C. Wilhelm, P. Stoyanov, and O.S. Es-Said

(Submitted January 2, 2008)

Aluminum and copper cylindrical shells were plastically buckled under quasi-static and dynamic loading conditions with an Absorption Compression-Torsion Plasticity (ACTP: Patent No. WO 2005090822) combined mechanical testing device. Optical microscopy and transmission electron microscopy (TEM) analysis were used to study the microscopic evolutions in the mechanically buckled aluminum and copper alloy samples. Optical microscopy showed evidence of the presence of second-phase particles in both the aluminum and copper alloys samples. Under dynamic loading aluminum samples showed more energy absorption as compared to copper samples. Material flow lines were more pronounced in the copper samples when observed by optical microscopy. The evidence that supports the increased energy absorption in the aluminum cylindrical shells can be supported by the TEM analysis more than the optical microscopy analysis. The TEM results showed highly oriented textured morphology with the presence of few dislocation cells structures and sub-structures.

Keywords ACTP, aluminum and copper alloys, cylindrical shells, quasi-static and dynamic plastic buckling

1. Introduction

The problem of safe vehicle design with maximum impact energy absorption is a significant subject in structural crashworthiness design. Original ideas in this field are still needed to thoroughly optimize the energy dissipating devises. The energy absorbed during plastic deformation is one of the major factors dealing with the energy dissipating systems. In the case of dynamic collapse of thin-walled cylindrical tubular structures, several recent studies (Ref 1-6) demonstrate that the mechanical behavior of such structures is strongly influenced by structural and material features, inertia, and strain rate effects. The dynamic axial crushing of the cylindrical tubes represents an efficient energy absorption system, which depends strongly on these mentioned key parameters. The complexity of the dynamic plastic buckling due to the coupling between the inertia effect and plastic properties of the collapsed material gives therefore highly non-linear dynamic structural parameters.

Under uniaxial plastic buckling, the plastic flow is always controlled by sequential compression and bending stresses, which constitute a complex load/unload path. Thus, the phenomenon of dynamic buckling proves, in general, a large sensitivity to the loading path, particularly in the plastic zone (Ref 7). On the other hand, under biaxial plastic buckling, the Absorption Compression-Torsion Plasticity (ACTP) testing device can generate a biaxial combined compression-torsion loading path from a uniaxial loading mode (Ref 8, 9), Fig. 1.

The philosophy of the ACTP device is based on a new idea aiming to simulate an extra-absorption of energy within a loaded structure by means of the loading path complexity concept. In fact, via such a device, the plastic strain becomes progressively complicated since a shear component is added to these sequential phases of compression and bending under dynamic loading. This means that three different strains (compression, bending, and shear) are concurrently applied with more complex load/unload condition. Simulated by the ACTP, several degrees of loading path complexity can also be created within the loaded specimens during their collapses. The behavior of the biaxially crushed materials has been studied demonstrating mainly the dependence of the plastic buckling on the specimen geometry, loading path complexity and its rate. Baleh and Abdul-Latif works (Ref 8, 9) investigated different tubular structures made from copper and aluminum alloys. Under dynamic loading, their results for aluminum tubular structures in biaxial–45° deformation mode showed an enhancement of 150% in energy absorption compared to the classical uniaxial deformation mode, Fig. 2(a). Figure 2(b) shows the different dynamic modes of loading complexities for the tested copper alloy cylindrical structures.

They also observed dynamically similar trend for copper tubular structures. The increase in the energy absorption, under quasi-static biaxial loading path (combined compression-torsion), attains up to 35% increase compared to the classical uniaxial case for the copper cylindrical shells. The energy absorption properties enhancement phenomenons of the tested materials are strongly affected by the loading path complexity.

N. Drusina, C. Wilhelm, P. Stoyanov, and **O.S. Es-Said**, Mechanical Engineering Department, Loyola Marymount University, Los Angeles, CA 90045-8145; **R. Mahapatra**, Naval Air Systems Command, Naval Air Warfare Center, Patuxent River, MD 20670-1908; and **A. Abdul-Latif** and **R. Baleh**, Laboratoire de Mécanique, Matériaux et Modélisation (L3M), Universite Paris 8, IUT de Trembaly, Paris, France. Contact e-mail: oessaid@lmu.edu.

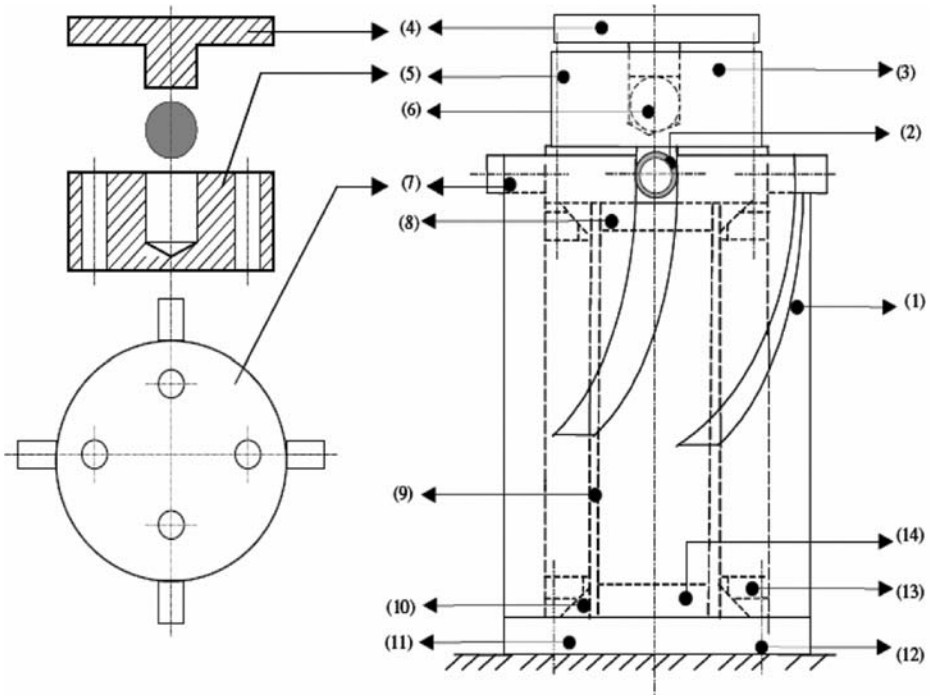

Fig. 1 The ACTP devices contains the following: (1) cylindrical body, (2) roller, (3) intermediate cylinder, (4) receiving disk, (5) higher tightening screw, (6) centering ball, (7) crosspiece, (8) higher disk, (9) specimen, (10) lower conical half-shells, (11) basic disk, (12) lower tightening screw, (13) lower conical clip, (14) lower disk (Ref 8, 9)

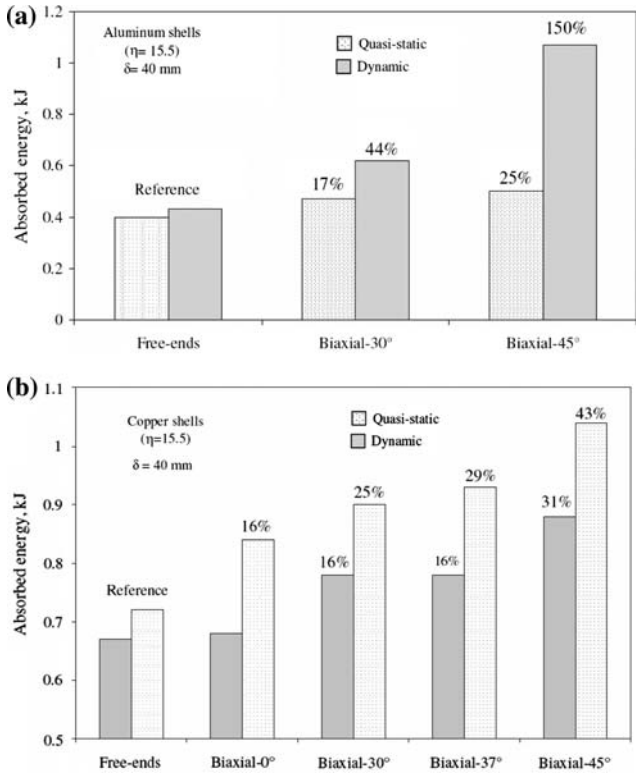

Fig. 2 (a) Different dynamic loading complexities for 6060 aluminum alloy, (Ref 9). (b) Different dynamic loading complexities for NFA5 1120copper alloy, (Ref 9)

When the higher biaxial loading complexity is applied; the greater is the energy absorbed by tubular structures made from copper and aluminum alloys.

The present work represents an extension of Abdul-Latif and Baleh works (Ref 8-10) and the objective is to relate the details of microstructural evolution to the uniaxial and biaxial deformation of these materials.

2. Experimental

2.1 Alloys

Tables 1 and 2 show the composition, in weight percentage, of the tubular aluminum alloy and the copper alloy used for this evaluation.

2.2 Metallography Experimental Procedure

The buckled samples were slowly cut with a silicon carbide saw blade. They were then mounted in a fast setting epoxy. The aluminum samples were etched with Keller's Reagent (95 mL H2O, 2.5 mL HNO3, 1.5 HCL, and 1.0 mL HF). The copper samples were etched with 50% HNO3 and 50% acetic acid. The microscope used was a Zeiss Axiovert 25 (50-500×). Optical microscopy was used to examine the different samples and photomicrographs were taken to document the observations.

2.3 TEM Experimental Procedure

Thin foil specimens for transmission electron microscopy (TEM) observations were obtained by electropolishing the

specimens in an electrolyte of 30 vol.% HNO_3 and 70 vol.% CH_3OH at 223 K using a Fischione Twin-Jet Electropolisher. The microstructure evolution due to uniaxial and biaxial buckling of copper and aluminum alloys was observed by using a JEOL JEM–2100, high-resolution transmission microscope operating at an accelerating voltage of 200 KeV.

3. Results and Discussions

3.1 Aluminum Alloy Buckling Results

The image of as-received tubular aluminum alloy (A50-451 (6060)) is shown in Fig. 3(a). Figure 3(b) shows the presence of second-phase particles in the matrix. Figure 3(c) and (d)

Table 1 Chemical composition

		Elemental composition										
Alloy		**Si**	**Fe**	**Cu**	**Mn**	**Mg**	**Cr**	**Zn**	**Ti**	**Other**	**Total**	**Al**
Aluminum A50-451 (6060)	Min.	0.3	0.1	...	0.1	...	...	...	...	...	...	Remainder
	Max.	0.6	0.3	0.1	0.35	0.6	0.05	0.15	0.1	0.05	0.15	...

Table 2 Chemical composition

		Elemental composition	
Alloy		**Cu**	**P**
Copper NFA51120	Min.	99.9	0.013
	Max.	...	0.05

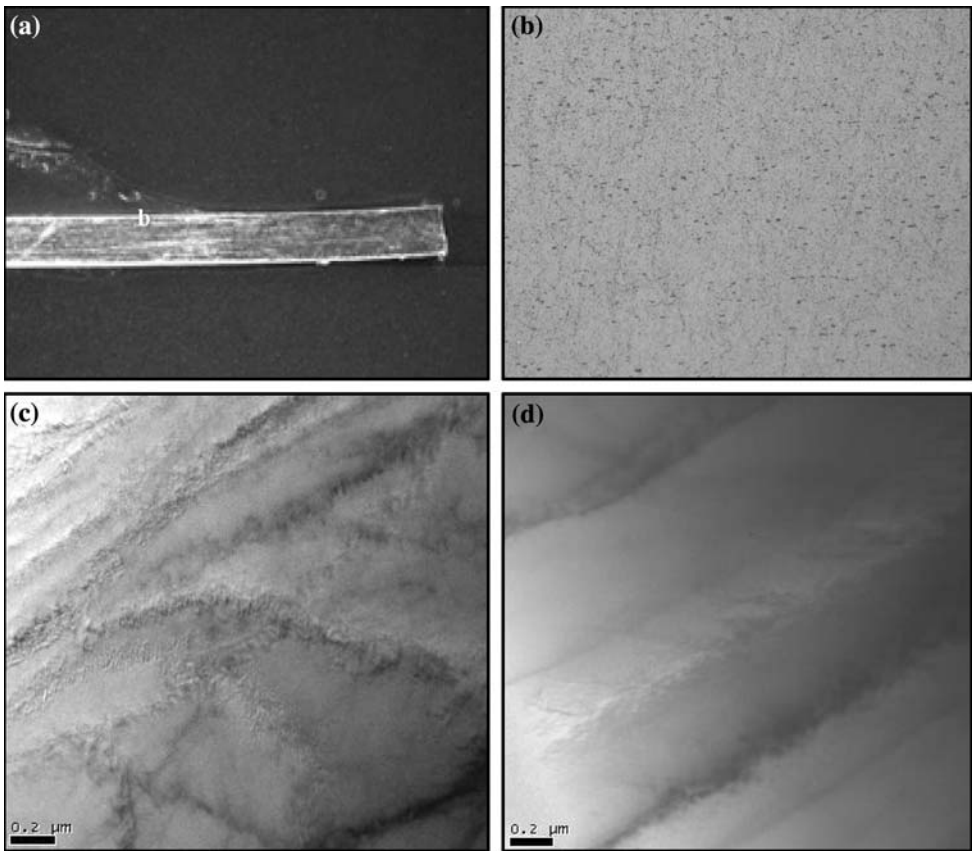

Fig. 3 (a) As-received aluminum with no buckling. (b) As-received aluminum with no buckling (200×). (c) As-Received TEM image of the microstructure demonstrating dislocation cell structure and sub-structure. (d) As-Received TEM image of the microstructure with evidence of oriented textured structure

show a highly oriented textured morphology, a few dislocation cell structures and sub-structures were also observed. Similar findings have been reported by Read and Johnson (Ref 11).

Figure 4(a-e) demonstrates the macro and microstructure results of the aluminum tubes buckled at a 37°. The buckled samples show uneven bends with areas with tension and compression. As the aluminum alloy is very soft, it was at times difficult to distinguish between the material moved during polishing or due to the buckling stresses. The tear of the right side of the material is more likely to have occurred by the polishing and not from the buckling stresses (Fig. 4c). The areas of compression (Fig. 4d and e) both show the stress cracks approximately 0.0127 cm (.005 inches) in length. Flow lines of the material are not as evident in this 37° buckled aluminum sample.

Figure 5(a-e) demonstrate the macro and microstructure of the aluminum tubes buckled at a 45°. The buckled samples also had uneven bends with areas of tension and compression. The areas of compression (Fig. 5b and d) both show the stress cracks. Flow lines of the material are not as evident in this 45° buckled aluminum sample.

Figure 6(a) and (b) are the TEM images of uniaxial deformed aluminum tube. High-density dislocation cells along with well-defined deformation bands in specific orientations were observed. The high-density tangled dislocations are sessile in nature. The increase in strength observed during uniaxial deformation mode by Abdul-Latif and Baleh (8-10) is related to these sessile dislocations.

Figure 6(c) and (d) show the TEM images of combined biaxial deformed aluminum tubular material. Unlike uniaxial deformation, the biaxial deformed specimen with 45° displays a predominately cellular microstructure with very high-density tangled dislocation network. This deformation mode is likely related to a mixed mode (XM) as reported by Abdul-Latif and Baleh (8-10). The presence of high-density tangled sessile dislocations explains the increase of 150% in the biaxially deformed (−45°) aluminum alloy.

3.2 Copper Alloy Buckling Results

Similar results in the copper macrostructure and microstructure were observed. Flow lines were more pronounced in the

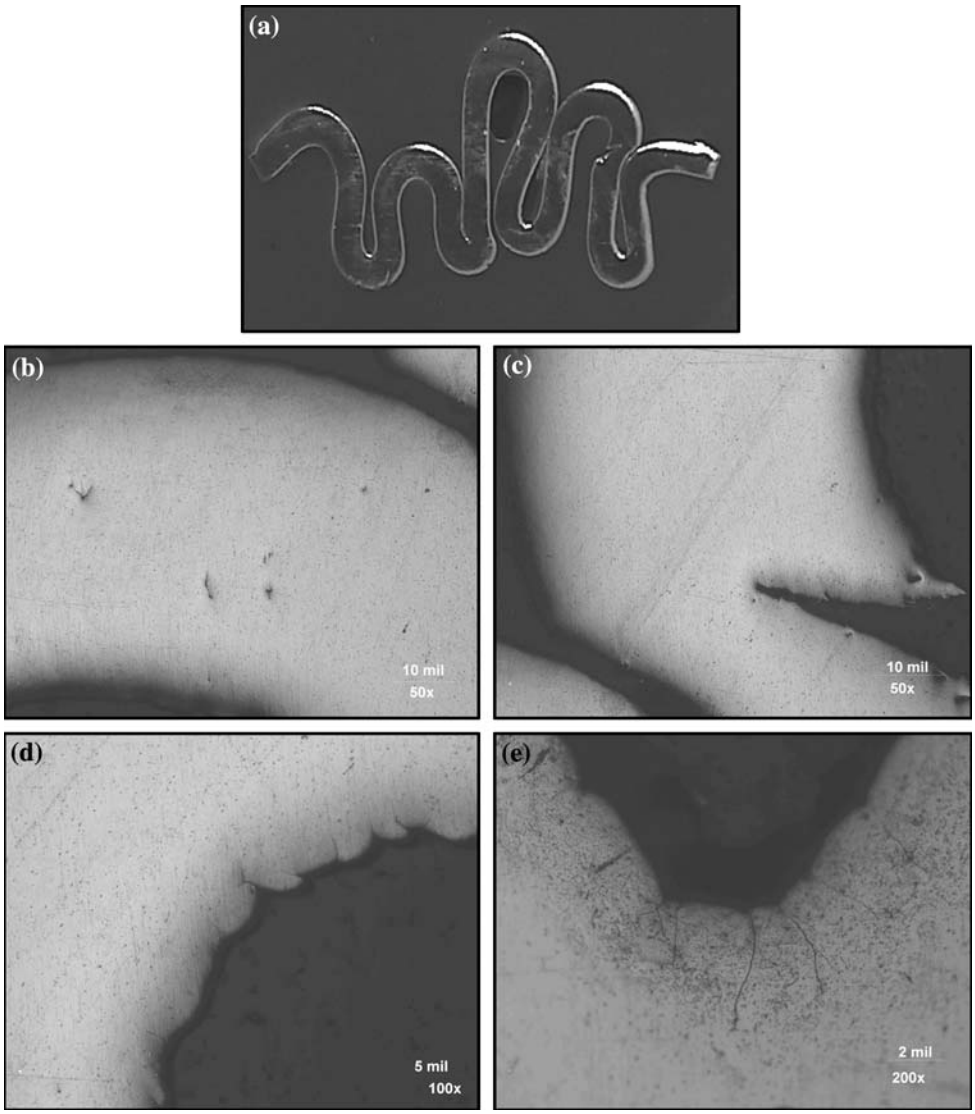

Fig. 4 (a) Aluminum sample biaxially buckled at a 37°. (b) Overall bend features (50×). (c) Material flow lines due to polishing (50×). (d) Compression stress cracks (100×). (e) Compression stress cracks (200×)

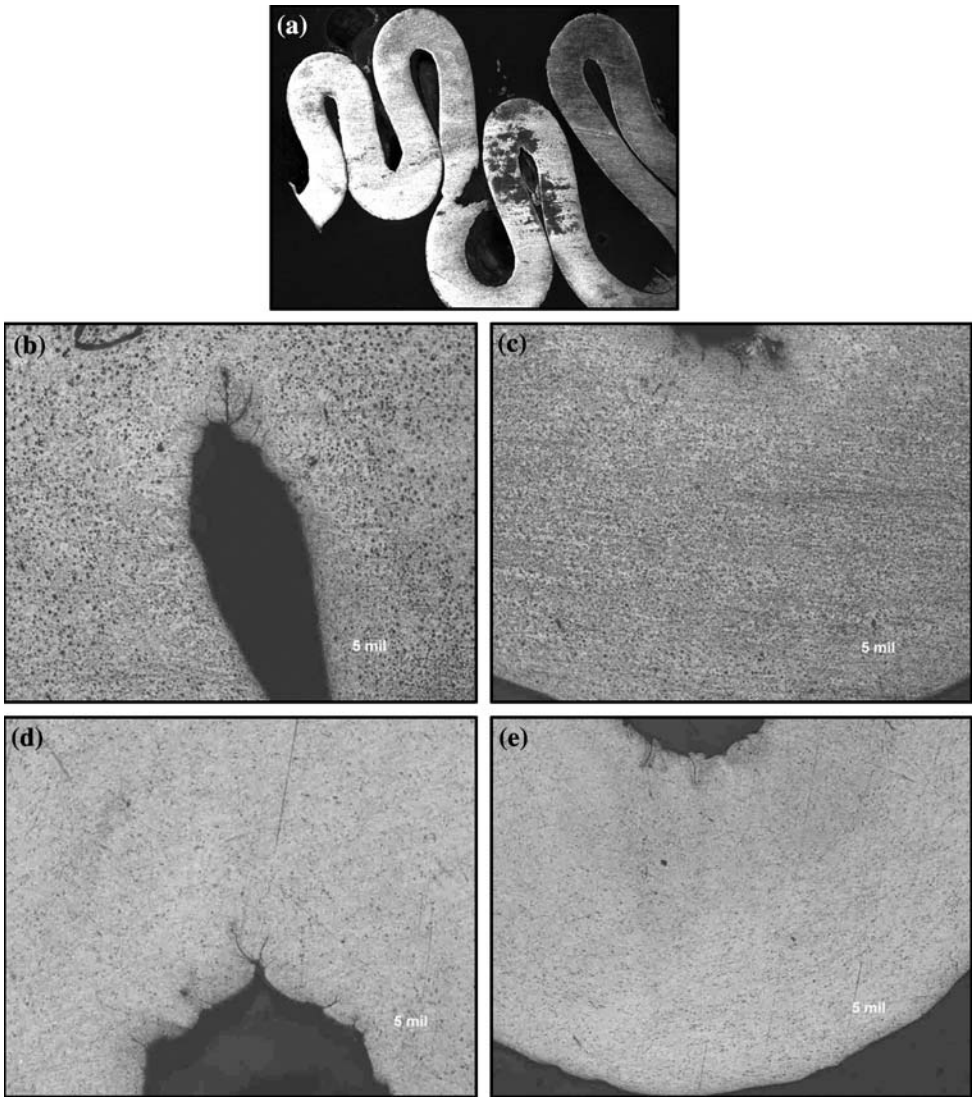

Fig. 5 (a) Aluminum sample biaxially buckled at a 45°. (b) Close up microstructure of the compressed portion of the aluminum crushed sample (50×). (c) Closed up microstructure of the bulk material of the aluminum crushed sample (50×). (d) Close up of the microstructure at the compressed portion of the aluminum crushed sample (50×). (e) Microstructure of the tension and compression portion of the crushed sample (50×)

copper samples than in the aluminum samples, Fig. 7(a), as compared to Fig. 3(b). The TEM images of as-received copper tube (NFA51120) are shown in Fig. 7(b) and (c). A textured microstructure and dislocation network were observed.

Figure 8(a-e) demonstrate the macro and microstructure results of the copper alloy tubes biaxially buckled at a 30°. The buckled samples show evenly distributed bends with areas with tension and compression. The areas of compression (Fig. 8b and c) both show the stress cracks with a maximum length of approximately 0.0064 cm (.0025 inches). Again, flow lines of the material are more pronounced in the copper samples as compared to the aluminum samples.

Figure 9(a-e) show the macro and microstructure results of the copper alloy tubes biaxially buckled at a 37°. The buckled samples show partially even distributed bends with areas with tension and compression. The areas of compression (Fig. 9b and c) both show stress cracks with a maximum length of approximately 0.008 cm (.003 inches). Flow lines of the material were also more pronounced in this 37° copper sample than in the aluminum samples.

Figure 10(a-e) show the macro and microstructure results of the copper alloy tubes biaxially buckled at a 30°. The areas of compression (Fig. 10b and c) both show the stress cracks with a maximum length of approximately 0.005 cm (.002 inches). Flow lines of the material were also more pronounced in this biaxial 30° copper sample than in the aluminum samples.

Figure 11(a-e) demonstrate the macro and microstructure results of the copper alloy tubes biaxially buckled at a 45°. The buckled samples show partially even distributed bends with areas with tension and compression. The areas of compression (Fig. 10b and c) both show the stress cracks with a maximum length of approximately 0.005 cm (.002 inches). Flow lines of the material were also more pronounced in this biaxial 45° copper sample than in the aluminum samples.

The TEM images of uniaxial deformed copper tubes are shown in Fig. 12(a) and (b). Deformation bands, fragmented grain and network of dislocations were clearly seen, indicative that the material was exposed to axisymetric severe plastic deformation. The increase in buckling strength in this mode is

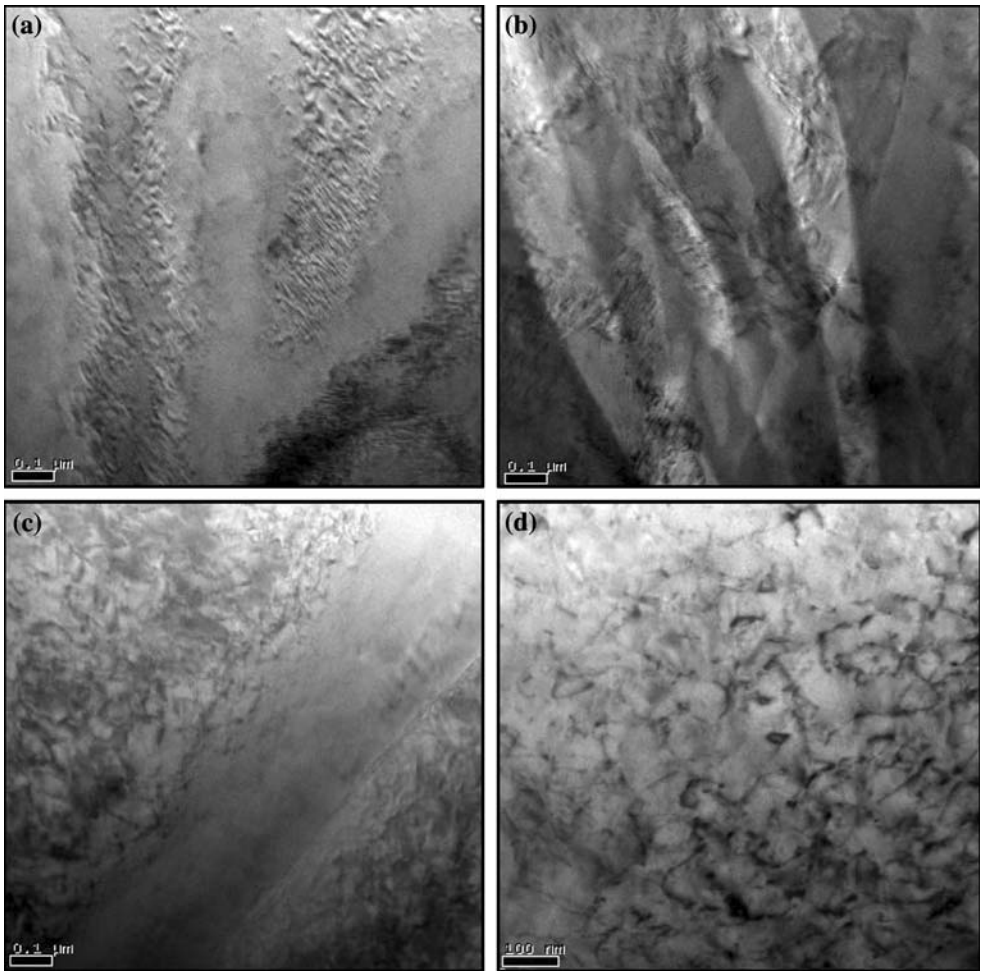

Fig. 6 (a) TEM image of uniaxial deformed aluminum alloy tube, with dislocation cell structures. (b) TEM image of uniaxial deformed aluminum alloy tube with deformation bands. (c) TEM image of biaxial deformed (–45°) aluminum alloy with evidence of deformation bands. (d) TEM image of biaxial deformed (–45°) containing a cellular structure

related to the presence of large density of sessile dislocations seen in the deformed structure.

The TEM images of biaxial deformed copper tube are shown in Fig. 13(a) and (b). The deformation mechanism seems to be quite different from that observed in uniaxially deformed specimens. Primary deformation mode appears to be due to twinning. Also, slip bands and dislocation networks were observed along with twins in some areas. Further study is continuing to elucidate the role of twins in the deformation mechanism of the biaxial deformed material.

4. Summary

The results of previous aluminum and copper evaluations demonstrated that the aluminum alloy absorbed the most energy up to 150% compared to the 35% by the copper. With the extended evaluation of the microstructure the conclusions are:

Aluminum alloy tubes contained:

- Second-phase particles in the aluminum matrix.
- Stress cracks were created in the compressed portions of the copper samples with maximum crack length was measured at 0.0127 cm (.005 inches).
- Material flow lines were not pronounced.
- TEM results demonstrate dislocation cells, substructures in the as-received sample, dislocation cells and deformation bends in the uniaxial sample and finally deformation bands and cellular structure in the biaxial sample.

Copper alloy tubes contained:

- Minimal second-phase particles in the copper matrix.
- Stress cracks were created in the compressed portions of the copper sample with a maximum crack length measured at 0.0076 cm (.003 inches).
- Material flow lines were very pronounced and flowed with the material movement.
- TEM results demonstrate textured structure, dislocation network and cells in the as-received sample, deformation bands and sub-structure in the uniaxial sample, and finally deformation bands, twins, and slips bands in the biaxial sample.

Acknowledgments

The authors wish to thank Mr. C. Kinney for his help with the metallographic preparation.

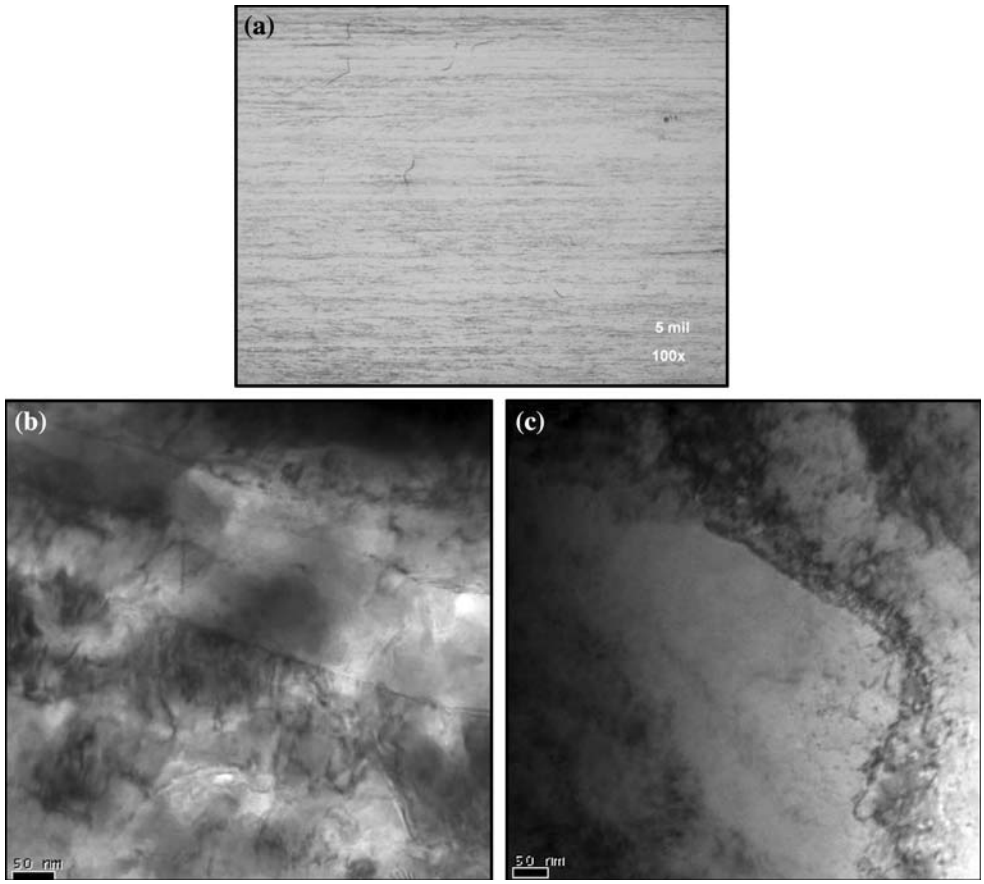

Fig. 7 (a) As-Received Copper sample with material flow lines (100×). (b) TEM image of as-received copper tube with textured structure and dislocation network. (c) TEM image of as-received copper tube with evidence of dislocation cells

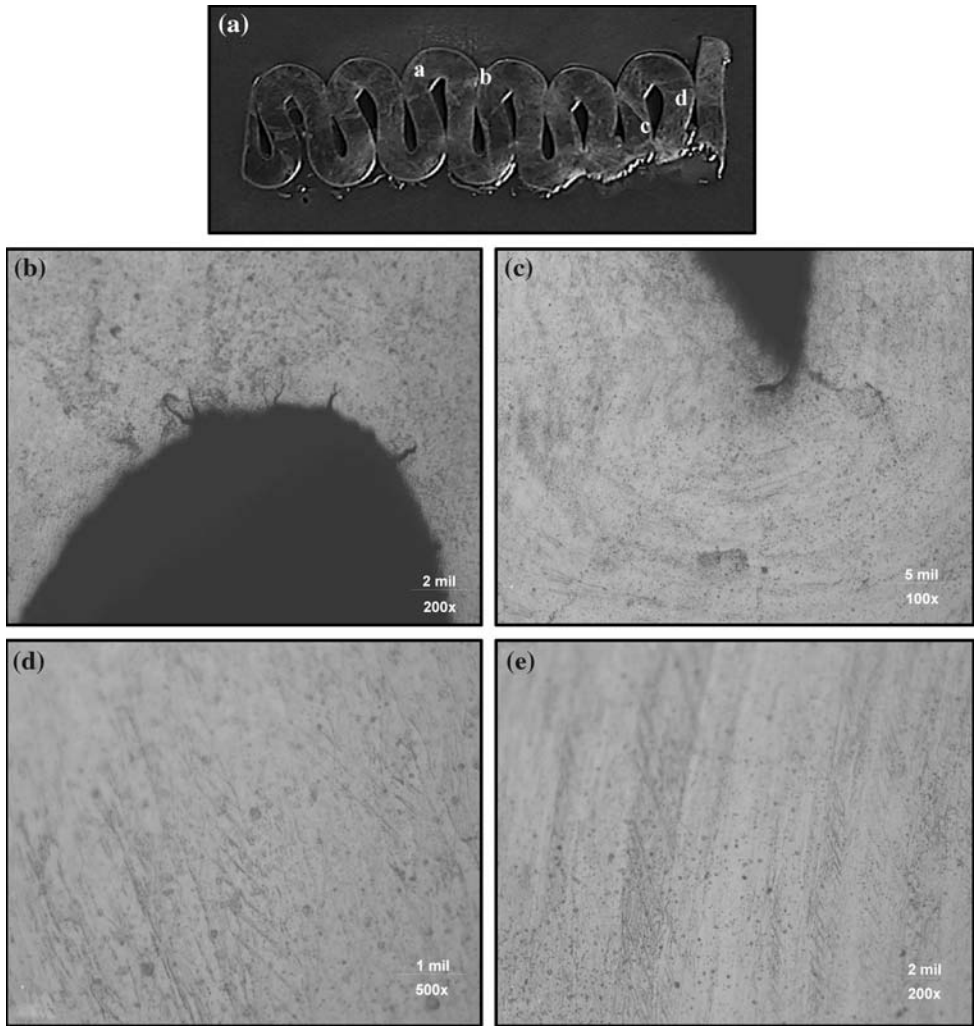

Fig. 8 (a) Biaxially buckled copper alloy sample at 30°. (b) Compression stress cracks (200×). (c) Compression stress cracks (100×). (d) Second-phase particles in the matrix (500×). (e) Another view of the second-phase particles in the matrix (200×)

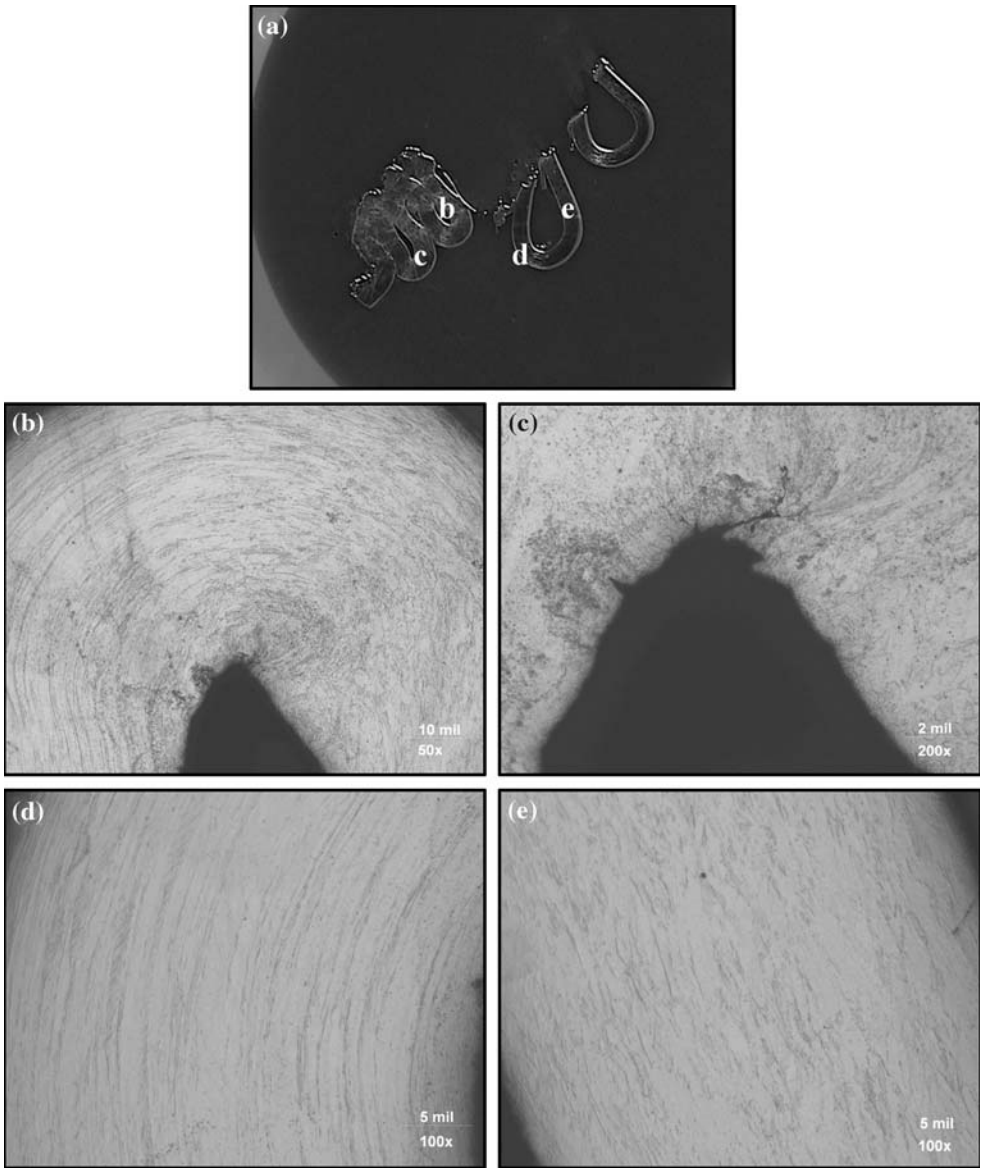

Fig. 9 (a) Biaxially buckled copper alloy sample at 37°. (b) Overall bend features (50×). (c) Compression stress cracks (200×). (d) Curved flow lines (100×). (e) Straightened flow lines (100×)

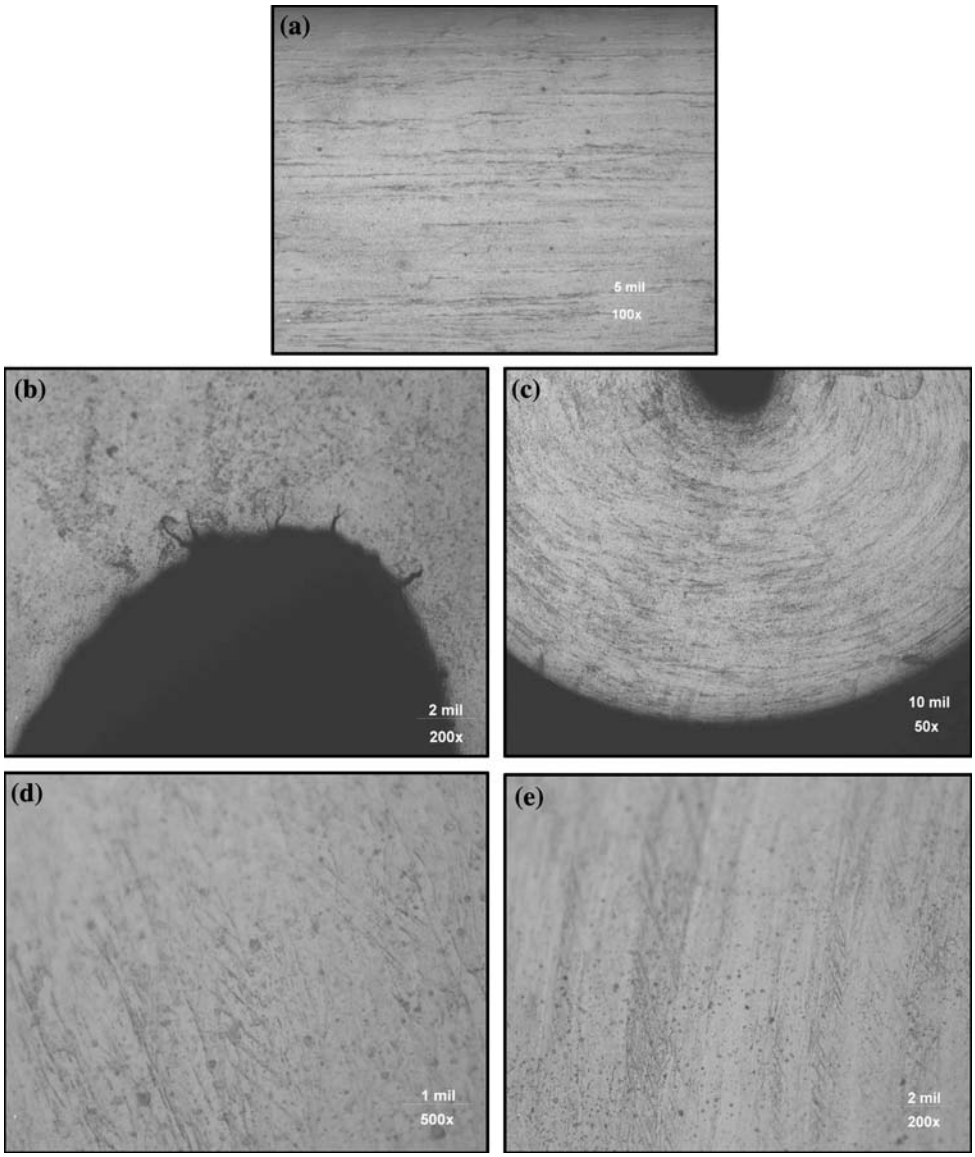

Fig. 10 (a) Biaxially buckled copper sample at 30° (100×). (b) Compression stress cracks (200×). (c) Tension and compression sides of the sample bend showing flow lines (50×). (d) Second-phase particles in the matrix (500×). (e) Another view of the second-phase particles in the matrix (200×).

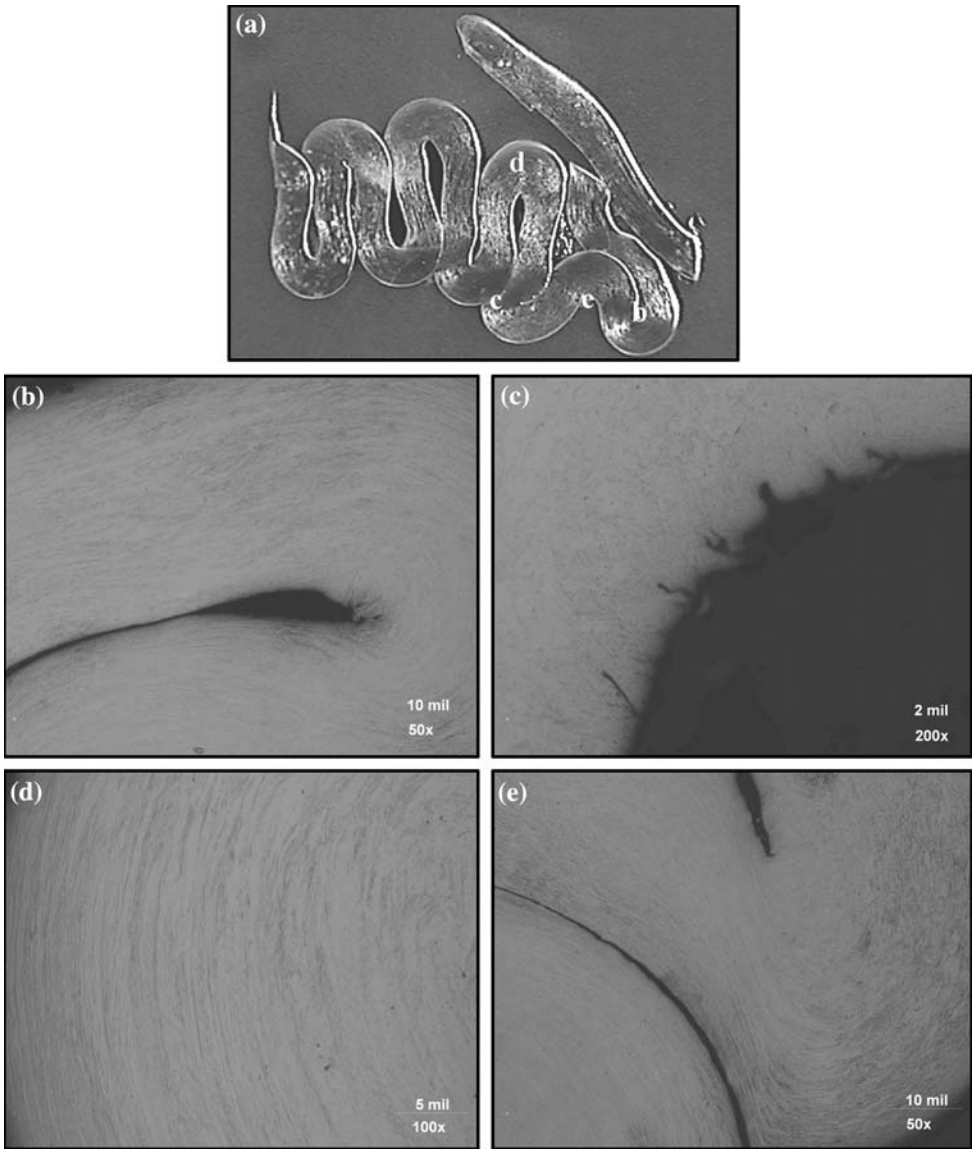

Fig. 11 (a) Copper sample biaxially crushed with a 45°. (b) Copper compressed microstructure (50×). (c) Microstructure shows evidence of flow lines and stress cracks (50×). (d) Copper microstructure bulk material flow lines (100×). (e) Compression area microstructure with stress cracks (200×)

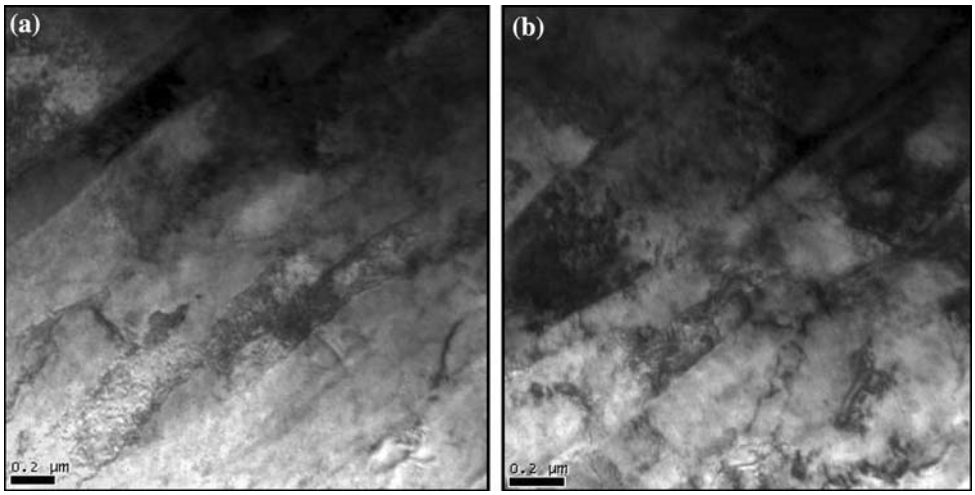

Fig. 12 (a) TEM image of uniaxial deformed copper tube demonstrated deformation bands. (b) TEM image of uniaxial deformed copper tube demonstrates dislocations and sub-structures

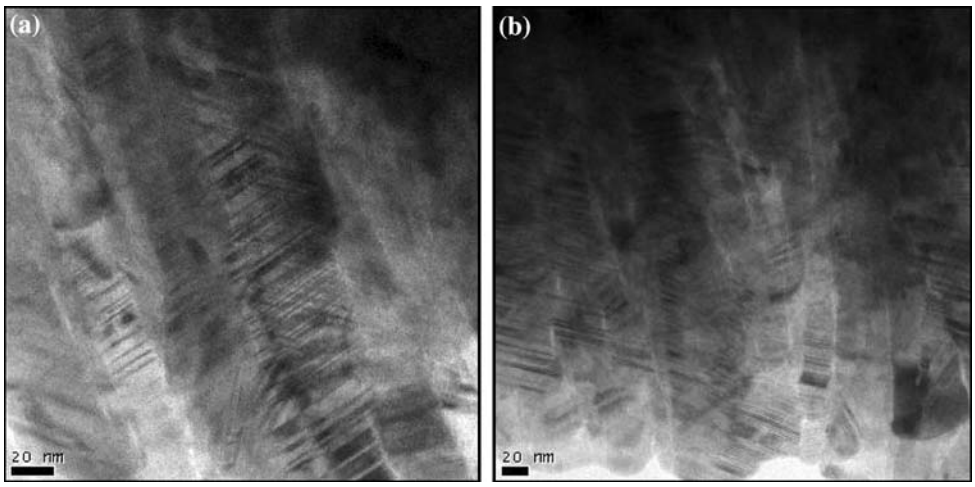

Fig. 13 (a) TEM image of biaxial deformed (−45°) copper tube: Deformation bands, Twins, and Slip bands. (b) TEM image of biaxial deformed (−45°) copper tube: Deformation bands, Twins, and Slip bands

References

1. C.R. Callandine and R.W. English, Strain-Rate and Inertia Effects in the Collapse of Two Energy Absorbing Structures, *Int. J. Mech. Sci.*, 1984, **26**, p 689–701
2. S.R. Reid, Plastic Deformation Mechanisms in Axially Compressed Metal Tubes Used as Impact Energy Absorbers, *Int. J. Mech. Sci.*, 1993, **35**, p 1035–1052
3. A.A.A. Al-Ghamdi, Collapsible Impact Energy Absorbers: An Overview, *Thin Walled Struct.*, 2001, **39**, p 189–213
4. N. Jones, Some Recent Developments and Future Trends in Thin-Walled Sections for Structural Crashworthiness, *Thin Walled Struct.*, 1998, **32**, p 231–233
5. D. Karagiozova and N. Jones, Dynamic Elastic-Plastic Buckling of Circular Cylindrical Shells Under Axial Impact, *Int. J. Solids Struct.*, 2000, **37**, p 2005–2034
6. D. Karagiozova and N. Jones, On Dynamic Buckling Phenomena in Axially Loaded Elastic-Plastic Cylindrical Shells, *Int. J. NonLinear Mech.*, 2002, **37**, p 1223–1238
7. D. Karagiozova and N. Jones, Dynamic Effects on Buckling and Energy Absorption of Cylindrical Shells Under Axial Impact, *Thin Walled Struct.*, 2001, **39**, p 583–610
8. R. Baleh and A. Abdul-Latif, Quasi-Static Biaxial Plastic Buckling of Tubular Structures Used as an Energy Absorber, *J. Appl. Mech.*, 2007, **74**, p 628–635
9. A. Abdul-Latif and R. Baleh, Dynamic Biaxial Plastic Buckling of Circular Shells, *J. Appl. Mech.,* 2007 (in press)
10. A. Abdul-Latif, R. Baleh, and Z. Aboura, Some Improvements on the Energy Absorbed in Axial Plastic Collapse of Hollow Cylinders, *Int. J. Solids Struct.*, 2006, **43**, p 1543–1560
11. W. Johnson and S.R. Reid, Metallic Energy Dissipating Systems, *Appl. Mech. Rev.*, 1986, **31**, p 277–288